# Nodes in the gap function of LaFePO, the gap function of the Fe(Se,Te) systems, and the STM signature of the $s_\pm$ pairing

Fa Wang,[1] Hui Zhai,[2] and Dung-Hai Lee[3,4]

[1]*Department of Physics, Massachusetts Institute of Technology, Cambridge, Massachusetts 02139, USA*
[2]*Institute for Advanced Study, Tsinghua University, Beijing 100084, China*
[3]*Department of Physics, University of California at Berkeley, Berkeley, California 94720, USA*
[4]*Materials Sciences Division, Lawrence Berkeley National Laboratory, Berkeley, California 94720, USA*

We reiterate, in more details, our previous proposal of using quasiparticle interference to determine the pairing form factor in iron-based superconductors. We also present our functional renormalization group (FRG) results on LaFePO and Fe(Se,Te) superconductors. In particular, we found that the leading pairing channel in LaFePO is nodal $s_\pm$ with nodes on electron Fermi surfaces. For Fe(Se,Te) system we found fully gapped $s_\pm$ pairing with substantial gap anisotropy on electron Fermi surfaces and large gap is concentrated in regions with dominant $xy$ orbital character. We further fit the form factor obtained by FRG to real-space orbital basis pairing picture, which shows more clearly the differences between different iron-based superconductors.

In the midst of many remaining issues of the iron-based superconductors, the "pairing symmetry" has attracted a lot of attention. From the theoretical side, the answer converged rather quickly to the $s_\pm$ form factor.[1–7] However, on the experimental side conflicting evidences exist for the presence of nodes[8] and full gap.[9] Note that we use "form factor" rather than pairing symmetry to describe $s_\pm$. This is because from the symmetry point of view there is no difference between the $s_\pm$ and the usual $s$-wave pairing. Indeed, under the action of the crystal point group, both transform as the identity (trivial) representation. This is in marked contrast with the $d_{x^2-y^2}$ pairing symmetry of the cuprates, which transforms as a distinct irreducible representation upon the point group operations. Thus while there is sharp (symmetry) distinction between the $d_{x^2-y^2}$ and the usual $s$-wave pairing, such distinction does not exist between $s_\pm$ and $s$. This is why phase sensitive measurements probing the relative phase of the superconducting order parameters residing in regions with different spatial orientation are ideal to rule in or rule out the $d_{x^2-y^2}$ pairing[10,11] while they cannot definitively prove or disprove the $s_\pm$ form factor.[12]

Nonetheless at this point there exist two types of proposed experiment which can address whether the gap function on the electron and hole pockets are indeed of opposite sign. Both of them provide information about the relative (spinor) phase of the quasiparticle wave functions on the electron and hole pockets. One of them is the detection of neutron resonance mode in the superconducting state. As suggested in Refs. 13 and 14, if the pairing form factor is $s_\pm$ one expects neutron resonance peaks at momenta $(\pm\pi,0)$, $(0,\pm\pi)$ to occur in the superconducting state. The energy location of the peaks is less than the sum of the minimum gaps on the electron and hole pockets. Interestingly the resonance peak has been observed.[15–19]

In a recent paper[20] the present authors proposed the second type of experiment—scanning tunnel microscope (STM) "quasiparticle-interference" experiment. This experiment can also probe the relative (spinor) phase between the quasiparticles on the electron and hole pockets. Here we repeat the

argument provided in Ref. 20. If the electron and hole Fermi surfaces have out-of-phase order parameters, the associated quasiparticle Nambu spinor will be orthogonal (left panel, Fig. 1).

For example, under the gauge where the order parameter is real, one of them will be $\sim(1,1)$, and the other $\sim(1,-1)$. The matrix elements of impurity-induced quasiparticle scattering from the hole to the electron Fermi surfaces (or vice versa) is nonzero/zero due to a scalar/magnetic impurity (which acts as the Pauli matrix $\sigma_z/I_{2\times2}$ in the Nambu space). The reverse is true for the scattering between two hole or two electron Fermi surfaces. As a result, if the main scattering source are scalar impurities, the quasiparticle interference peaks associated with $(\pm\pi,\pm\pi)$ (which arise from the scattering between two electron or two hole pockets, note that throughout this paper the "unfolded" zone notation of mo-
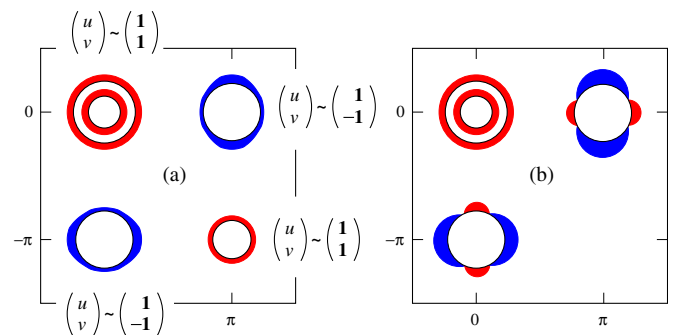


FIG. 1. (Color online) (a) Schematic representation of the $s_\pm$ pairing form factor and the associated quasiparticle Nambu spinors. Solid black circles represent the normal-state Fermi surfaces. Thickness of colored region around Fermi surfaces indicate magnitude of the gap $|\Delta(\mathbf{k})|$. Blue means positive and red means negative. The two component column vectors are the quasiparticle spinor wave functions associated with different Fermi surfaces. (b) A schematic representation of the pairing form factor for LaFePO obtained by FRG. There are four nodes of gap around each electron Fermi surface.

mentum space will be used) will be suppressed for bias close to the superconducting gap. In contrast, for magnetic impurity scattering, the quasiparticle interference peak around $(\pm\pi,0)$ and $(0,\pm\pi)$ (which correspond to the scattering between an electron and a hole pocket) will be suppressed. The contrast between these two sets of quasiparticle interference peaks should diminish as the bias is increased/decreased from the gap because the spinor phase of the quasiparticle wave functions are no longer solely determined by the gap parameter. The quasiparticle interference idea[21] has been developed into a fruitful spectroscopy of studying the cuprates.[22] It has also been used as a method to infer the pairing symmetry by Hanaguri *et al.*[23] In a recent beautiful STM experiment[24] done on the $Fe_{1+x}(Se,Te)$ compounds, the authors control the relative degree between scalar and magnetic impurity scattering by changing the density of superconducting vortices (which act as magnetic scattering centers). Interestingly the above behavior is observed.

Combining the neutron and the STM experiment it is fair to say that the evidences for the $s_{\pm}$ pairing is strong. The purpose of the present paper is to tie up the loose ends on the theoretical side. We study the pairing form factors for LaFePO and Fe(Se,Te) systems. These systems exhibit superconductivity without charge doping and are presumably less prone to disorder effects. LaFePO, among all iron-based superconductors, shows the strongest evidence for the existence of gap nodes.[25,26] For FeSe, there have been contradicting reports of nodeless[27] and nodal[28] superconductivities, as in many of its pnictides relatives. Bulk FeTe is not superconducting but becomes superconductor under tensile stress as thin films.[29]

We apply the functional renormalization group (FRG) method to study the pairing form factor. In particular, we incorporate the realistic band structures of these materials in the form of tight-binding models. We then transform the real-space on-site interaction into two-particle scattering vertex functions defined in the band eigenfunction basis. It turns out that much of the differences between the pairing form factors of LaFePO, Fe(Se,Te), and the LaFeAsO systems originate from the differences in the Fermi-surface topology as well as the orbital contents of the band wave functions. Thus the realistic band structure is indispensable for our purposes.

As pointed out in Refs. 30 and 31, the scattering vertex function acquires important angle dependence around the Fermi pockets due to the change in the orbital content of the band wave functions around each Fermi surfaces, and this can induce strong variation in the $s_{\pm}$ gap function around the electron pockets. Recently it has also been shown that a particular type of angular-dependent scattering amplitude can even lead to nodal $s_{\pm}$ form factor.[32–34]

The Hamiltonian we start with is given by the sum of the band structure part and the interaction part $H=H_0+H_{int}$. Because the relevant bands are mostly iron in character, we follow the literature in using a tight-binding model consists of only the iron orbitals. Moreover we focus on the two-dimensional $X$-Fe-$X$ ($X=As,P,Se$) trilayer in which the Fe form a square lattice. For both materials five-orbital tight-binding models in Eq. (1) fitted to the band structure are used

$$H_0 = \sum_{\mathbf{r},s}\sum_{ij}\sum_{a,b} t_{ij}^{ab} c_{ias}^{\dagger} c_{jbs}, \qquad (1)$$

where $a,b=1,5$ label the five Wannier $d$-orbitals ($3z^2-r^2,xz,yz,x^2-y^2,xy$) of Fe. Here $s=\uparrow,\downarrow$ labels spin, $i,j$ labels the iron sites. In the above $x$ and $y$ refer the two orthogonal Fe-Fe directions. After a staggered definition of the phase of the $xz$ and $yz$ orbitals, the tight-binding Hamiltonian can be made to have the translation symmetry consistent with one Fe per unit cell. In the rest of the paper we shall use this unit cell and the associated Brillouin zone (which is referred to as the "unfolded zone" in the literature).

For $H_{int}$ we only consider the following on-site interactions:

$$H_{int} = \frac{1}{2}\sum_{i}\sum_{s,s'}\left[\sum_{a,b} U_{ab} c_{ias}^{\dagger} c_{ibs'}^{\dagger} c_{ibs'} c_{ias} \right.$$
$$\left. + \sum_{a\neq b} J_{ab}:(c_{ias}^{\dagger} c_{ibs} + \text{H.c})(c_{ibs'}^{\dagger} c_{ias'} + \text{H.c.}):\right]. \quad (2)$$

Where :: means normal ordering, H.c. means hermitian conjugate of the previous term. When the parameters are available, we have studied the full-orbital-dependent interaction.[35] However in the rest of the paper we shall focus on the simpler case where $U_{aa}=U$ and $U_{ab}=U'$ for $a\neq b$, and $J_{ab}=J$ for $a\neq b$. For cases where the orbital-dependent interaction parameters are available we have checked that the above simplification does not change the qualitative nature of the results. The functional renormalization-group procedure and result analysis exactly follow that used in previous papers by the same authors,[5,20,31] except that we have achieved slightly better momentum resolution in the present work. In the following we present the results for LaFePO, FeSe, and FeTe separately.

## I. LaFePO

For LaFePO there is a discrepancy between the results of quantum-oscillation experiment[36] and the band-structure calculations.[32,37] While the band-structure calculations predict the presence of a three-dimensional (3D) $3z^2-r^2$ orbital holelike Fermi surface centered around $\mathbf{k}=(\pi,\pi,\pi)$, the quantum-oscillation experiment did not observe it. In our study we follow the quantum-oscillation experiment and adapt a band-structure model where there is only two-dimensional-like Fermi surfaces associated with the two hole pockets around $\mathbf{k}=(0,0)$ and two electron pockets around $\mathbf{k}=(\pi,0)$ and $(0,\pi)$, respectively. It is important to note that unlike the hole-doped 122 compounds, there is no two-dimensional $xy$ orbital character hole pockets centered at $\mathbf{k}=(\pi,\pi)$ (see Fig. 2, left panel). We shall also comment on why we do not believe the existence of the $(\pi,\pi,\pi)$ hole pocket from the theoretical perspective.

The FRG flow of the interaction associated with pairing and the $(\pi,0)$ spin-density wave (SDW) are shown in the middle panel of Fig. 2. (Strong negative interaction implies ordering instability.) Despite the fact that at high energies the SDW interaction is more negative, the superconducting pairing overwhelms the SDW interaction at low-energy cutoffs.
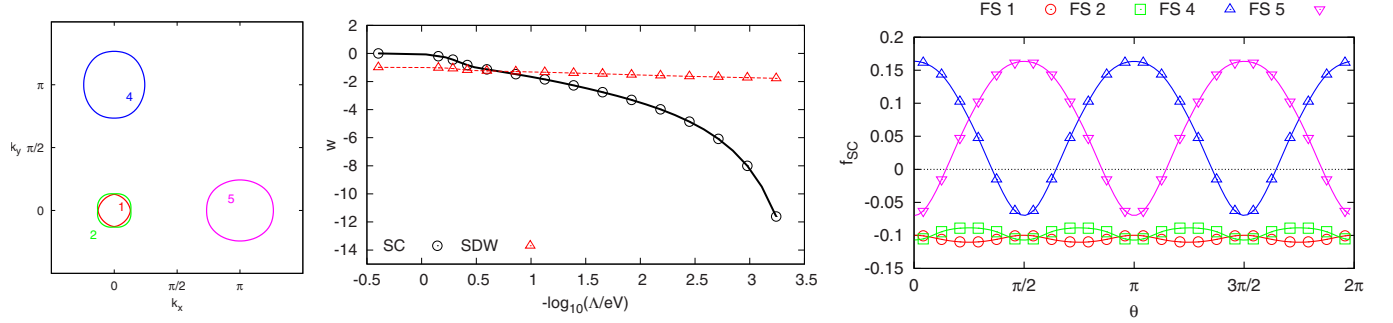
FIG. 2. (Color online) Left panel: the $k_z=0$ Fermi surfaces of LaFePO. Middle panel: the FRG flow of the interaction strength associated with the $(\pi,0)$ SDW and the superconducting pairing. $\Lambda$ is the energy cutoff. Right panel: the pairing form factor. The horizontal axis $\theta$ is the polar angle of Fermi-surface points with respect to the center of each Fermi surface. $\theta=0$ means $+k_x$ direction from the center of the Fermi surface. This notation will be used throughout this paper.

In the right panel of Fig. 2 we present pairing form factors associated with the four Fermi surfaces in the left panel. We note the following two facts. (1) The pairing form factor on each electron Fermi surface has four nodes. This is schematically represented in the right panel of Fig. 1(b). (2) The mean-gap function on the electron pockets has opposite sign from that on the two $\Gamma$ hole pockets. Hence it is justified to call them $s_\pm$ pairing. The presence of gap nodes on the electron pocket is consistent with the observation of the linear-$T$ dependent penetration depth.[25,26]

Next we address the issue of the absence/presence of the 3D hole pocket around $(\pi,\pi,\pi)$, i.e., the conflict between the quantum-oscillation experiment and the band-structure results. A cross section of the band-structure calculation results at $k_z=\pi$ is shown in the left panel of Fig. 3. The Fermi surface 3 is the controversial hole pockets. It is primarily made up of the $3z^2-r^2$ orbital. The rest of Fermi surfaces are connected to those at $k_z=0$ without significant dispersion. Our FRG result shows that while the bare pair scattering between the electron and the $3z^2-r^2$-like hole pocket is appreciable, as the energy cutoff is progressively lowered, such pair scattering diminishes. This is shown in the right panel of Fig. 3, where the black diamond symbols mark the form factor on the 3 Fermi surface—it is vanishingly small.[38] Clearly if this ungapped Fermi surface exists, it would change the temperature dependence of the penetration depth entirely. Thus we support the quantum-oscillation results and believe that the $(\pi,\pi,\pi)$ hole pocket is absent in LaFePO.

This makes the band structure of LaFePO essentially two-dimensional like the other 1111 and 122 compounds.

## II. FeSe

Experimental samples of FeSe usually contain small amount of excess Fe. But they are experimentally shown as nonessential or even destructive to superconductivity[39] and will be ignored in our study. The Fermi surface of the FeSe tight-binding model is shown in Fig. 4. Like the doped 122 systems there are two hole pockets centered around **k** $=(0,0)$, two electron pockets around **k**$=(\pi,0),(0,\pi)$, and one hole pocket around **k**$=(\pi,\pi)$.

The FRG flow of the interaction associated with pairing and the $(\pi,0)$ SDW are shown in the middle panel of Fig. 4. Again, while the SDW interaction is stronger (more negative) at high energies, it is surpassed by the superconducting pairing as the energy cutoff is lowered. In the right panel of Fig. 4 we present pairing form factors associated with the five Fermi surfaces in Fig. 4. We note the following facts. (1) The Fermi-surface shapes and orbital contents (not shown) are very similar to that of LaFeAsO. (2) The gap function on the two central hole pockets is quite small compared with that on the $(\pi,\pi)$ hole pocket (mainly $xy$ orbital) and the electron pockets. This suggests the main pairing source is the Cooper scattering between the $(\pi,\pi)$ hole pocket and the electron pockets. (3) The gap on the electron pockets has substantial variation similar to our previous results for the
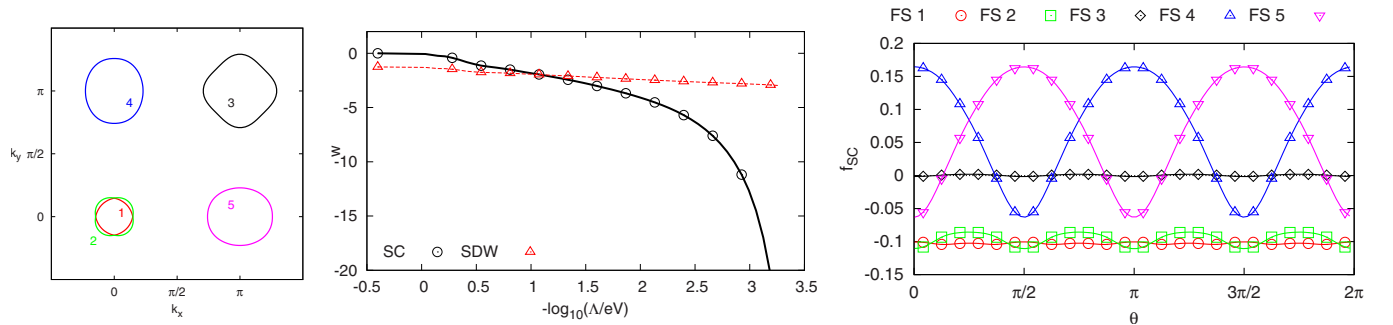


FIG. 3. (Color online) Left panel: the Fermi surfaces of LaFePO at $k_z=\pi$. Middle panel: the FRG flow of the interaction strength associated with the $(\pi,0)$ SDW and the superconducting pairing. Right panel: the pairing form factor determined by FRG.
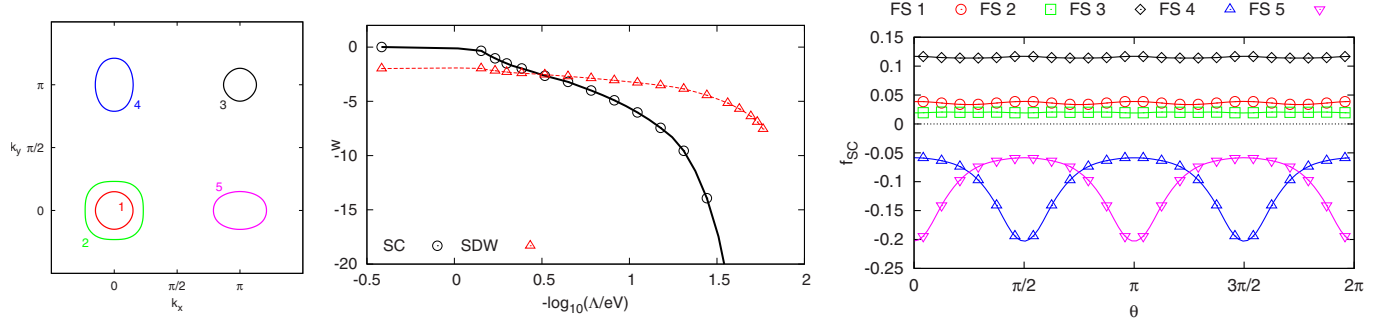
FIG. 4. (Color online) Left panel: the Fermi surfaces of FeSe. Middle panel: the FRG flow of the interaction strength associated with the $(\pi,0)$ SDW and the superconducting pairing. Right panel: the pairing form factor.

1111 systems.[5] However in this case the large gap is concentrated in regions with dominant $xy$ orbital content, i.e., the portion of electron Fermi surfaces facing the central hole pockets. This is different from our previous result of LaFeAsO where the $xy$ orbital dominant part of Fermi surfaces has minimal gap. (4) The gap function takes on opposite sign between the electron and hole pockets. Hence the pairing form factor is $s_\pm$. This is consistent with STM quasiparticle interference results of Hanaguri *et al.*[24]

## III. FeTe

Bulk FeTe is not superconducting and shows a different antiferromagnetic (AFM) order than the parent iron pnictides.[40] Its optical conductance does not show a clear Drude peak and does not exhibit a significant change across magnetic transition.[41] The magnetic moment in AFM state is large, about two Bohr magneton.[40] All these facts indicate that FeTe may be very different from FeSe and iron pnictides, and probably more strongly correlated. However upon Se substitution of Te superconductivity appears. Interestingly, in those superconducting samples neutron scattering shows broadened $(\pi,0)$ and $(0,\pi)$ peaks similar to those of the 122 family. This provides circumstantial evidences that the $(\pi,0)$ and $(0,\pi)$ magnetic scattering is tied to the superconducting pairing. Recently superconductivity in FeTe thin films under tensile stress was also reported[29] without Se substitution. Knowing the magnetic properties of the superconducting Fe(Se,Te) systems it is reasonable to expect that these film to exhibit $(\pi,0)$, $(0,\pi)$ antiferromagnetic correla-

tion rather than the $(\pi/2,\pi/2)$ antiferromagnetic correlation in bulk FeTe samples. Since the $(\pi,0)$, $(0,\pi)$ antiferromagnetic scattering is natural from the band structure point of view, it is reasonable to start from the itinerant picture when studying the superconductivity in FeTe films.

We use the tight-binding model fitted to the band-structure calculations for FeTe. The band structure has been partly confirmed by angle resolved photoemission spectroscopy (ARPES) measurement.[42] Although it does not capture the unusual magnetism in bulk FeTe, we hope it is an appropriate starting point to study the superconductivity in the FeTe thin films. Excess iron exists in experimental samples of FeTe as in the case of FeSe but will be ignored in our study. The Fermi surface, FRG flow and pairing form factor are presented in Fig. 5. As expected our results only show the $(\pi,0)$ SDW correlation, not the $(\pi/2,\pi/2)$ AFM in bulk FeTe.

We note the following facts: (1) the Fermi surface shapes and their orbital contents (not shown) are very similar to that of LaFeAsO, except that the small hole pocket at $\Gamma$ is much smaller, and has mainly $xy$ orbital character. (2) The gap on electron pockets has substantial variations but does not change sign. Like FeSe the large gap is concentrate in regions with dominant $xy$ orbital content. (3) The gaps on $(\pi,\pi)$ hole pocket is large and has opposite sign from that on the electron pockets. Like FeSe, this suggests the root of pairing rests on the Cooper scattering between the $(\pi,\pi)$ hole pocket and the electron pockets. (4) Interestingly, the gaps on the two central hole pockets are relatively small and have opposite sign. This suggests that these hole pockets play a secondary role in the superconducting pairing. The
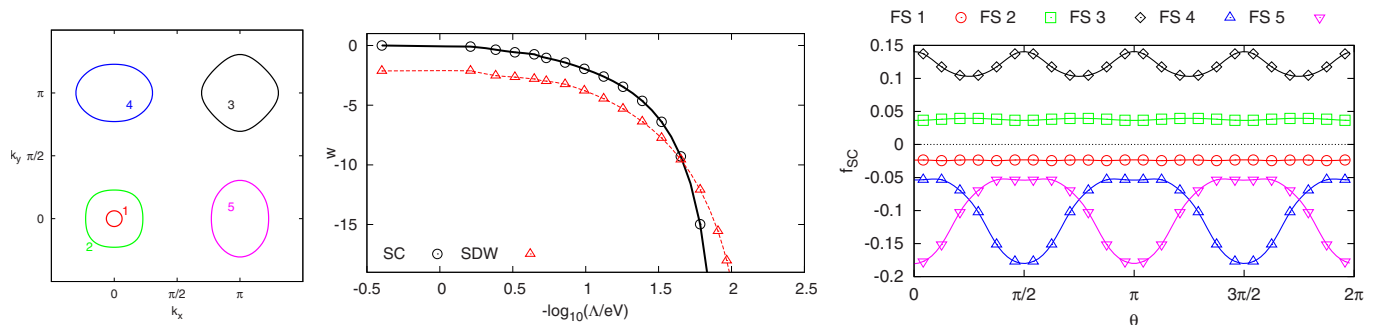


FIG. 5. (Color online) Left panel: Fermi surfaces of FeTe. Middle panel: the FRG flow of the interaction strength associated with the $(\pi,0)$ SDW and the superconducting pairing. Right panel: the pairing form factor determined by FRG.

fact that the gap function reverse sign on the central hole pockets is a new feature that is absent in other iron-based superconducting compounds.

## IV. REAL-SPACE REPRESENTATION OF THE PAIRING FORM FACTORS

Our FRG method can only calculate the pairing form factors around Fermi surfaces and the pairing order parameter is obtained in band eigenbasis. To gain more intuitive picture, it is useful to have a real-space picture of the pairing.

Based on our experience and other theoretical works, we will focus on only the three $t_2$ orbitals $Xz, Yz, xy$ (here capital $X, Y$ refer to the Fe-As directions, namely proper crystal axis) in the pairing order parameter. Off-site pairing between these three orbitals up to second neighbor on the Fe square lattice is included. According to the lattice symmetry the pairing order parameter has the following form:

$$\Psi^T_{-\mathbf{k},\downarrow} \begin{pmatrix} \Delta_{11}(k_x,k_y) & \Delta_{12} & \Delta_{13}(k_x,k_y) \\ \Delta_{12} & \Delta_{11}(k_y,-k_x) & \Delta_{13}(k_y,-k_x) \\ -\Delta_{13}(k_x,k_y) & -\Delta_{13}(k_y,-k_x) & \Delta_{33} \end{pmatrix} \Psi_{\mathbf{k},\uparrow},$$
$$(3)$$

where $\Psi^T_{-\mathbf{k},s} = (ic_{Xz,-\mathbf{k},s}\ ic_{Yz,-\mathbf{k},s}\ c_{xy,-\mathbf{k},s})$, superscript $T$ means transpose, $s = \uparrow, \downarrow$ labels the spin, $i = \sqrt{-1}$, and the entries of the matrix are

$$\Delta_{11}(k_x,k_y) = \Delta^\sigma \cos(k_x - k_y) + \Delta^\pi \cos(k_x + k_y) + \Delta^{(nn)}(\cos k_x + \cos k_y),$$

$$\Delta_{12} = -\Delta_{12}(\cos k_x - \cos k_y),$$

$$\Delta_{13}(k_x,k_y) = \Delta_{13}^{(nn)}(\sin k_x - \sin k_y) + \Delta_{13}^\sigma \sin(k_x - k_y),$$

$$\Delta_{33} = \Delta_{33}^{(nn)}(\cos k_x + \cos k_y) + \Delta_{33}^{(nnn)}\cos k_x \cos k_y.$$

The pictorial representation of the eight fitting parameters $\Delta^\sigma$, $\Delta^\pi$, $\Delta^{(nn)}$, $\Delta_{12}$, $\Delta_{13}^{(nn)}$, $\Delta_{13}^\sigma$, $\Delta_{33}^{(nn)}$, and $\Delta_{33}^{(nnn)}$ are illustrated in Fig. 6.

We then project this order parameter onto the Fermi surfaces and compare with the FRG results. The fitting parameters are obtained by standard least-square fit and listed in Table I. A similar real-space representation was recently obtained by Kariyado and Ogata from RPA results.[43] Note that although we have 24 points around one Fermi surface, due to the
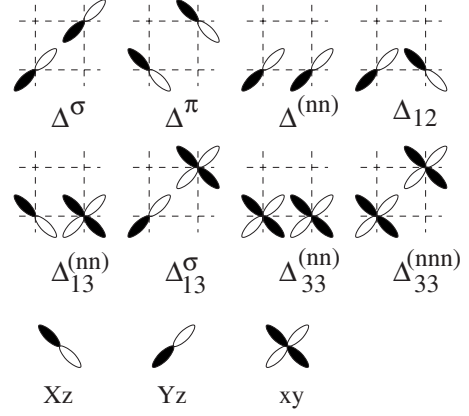


FIG. 6. Pictorial representation of the fitting parameters and the three orbitals used. Empty and filled lobes in the orbital pictures indicate $\pm$ sign/symmetry of wave functions. Each of the fitting parameters, $\Delta s$, represents spin-singlet pairing between the two orbitals shown in the corresponding picture.

$C_{4v}$ symmetry of our model, there are actually only 24/8 = 3 independent data points to fit per Fermi surface. At this stage we have not been able to improve this due to limitation of computational power. The fitting to LaFePO and FeSe are not very good with large error estimates. This could come from our limited momentum space resolution or that the pairing in these materials actually extend beyond second neighbor. So these results should be taken with caution.

Nonetheless the differences between these materials are clearly visible and are summarized below. (1) For LaFeAsO the intraorbital pairing ($\Delta^\sigma$ and $\Delta^{(nn)}$), between $Xz$-$Xz$ or $Yz$-$Yz$, are strongest, therefore the gap is smallest in regions with dominant $xy$ character.[5] (2) For LaFePO, the nearest-neighbor pairings, interorbital $\Delta_{12}$ between $Xz$-$Yz$, and intraorbital pairing $\Delta_{33}^{(nn)}$ between $xy$-$xy$, are the strongest, which give a nodal $\cos(k_x) + \cos(k_y)$ gap. (3) In FeSe the gap is mainly from intraorbital second-neighbor $xy$-$xy$ pairing $\Delta_{33}^{(nnn)}$, which gives $\cos(k_x)\cos(k_y)$-type nodeless gap. The gap variation on electron pockets is mainly due to the variation in $xy$ orbital content of the wave function. Thus it has the opposite anisotropy compared to our LaFeAsO result. (4) FeTe is very special, with dominant interorbital pairing ($\Delta_{12}$ and $\Delta_{13}^{(nn)}$) between $Xz$-$Yz$ and $Xz/Yz$-$xy$. The sign structure and variation in gap is a consequence of both this fact and the orbital content of the wave functions around Fermi surfaces.

TABLE I. Fitting parameter for different materials (dopings). The row of "LaFeAsO $n$=6.1" is for LaFeAsO model with 6.1 electrons per site. Others are "undoped" (6 electrons per site). Numbers in bracket are error estimate of the least-square fit. Note that the overall scale and sign are unimportant here.

| | $\Delta^\sigma$ | $\Delta^\pi$ | $\Delta^{(nn)}$ | $\Delta_{12}$ | $\Delta_{13}^{(nn)}$ | $\Delta_{13}^\sigma$ | $\Delta_{33}^{(nn)}$ | $\Delta_{33}^{(nnn)}$ |
|---|---|---|---|---|---|---|---|---|
| LaFeAsO $n$=6.1 | 0.216(7) | 0.085(8) | −0.20(2) | −0.15(1) | −0.05(2) | 0.021(6) | −0.013(6) | 0.03(1) |
| LaFePO | −0.10(7) | 0.08(3) | 0.08(4) | 0.4(1) | −0.2(2) | 0.09(3) | 0.4(4) | 0.3(2) |
| FeSe | 0.0(2) | 0.0(2) | −0.0(2) | −0.00(7) | 0.07(7) | 0.1(1) | 0.14(6) | 0.4(1) |
| FeTe | −0.11(4) | 0.14(3) | −0.02(6) | 0.31(9) | −0.25(3) | 0.12(6) | −0.01(2) | −0.06(1) |

## V. CONCLUSION

We have so far studied the pairing of LaFeAsO, LaFePO, FeSe, and FeTe (thin film) using the function renormalization-group method. The most robust picture that emerge from these studies is that pairing is due to the strong positive Cooper scattering between the hole and electron Fermi surfaces. The positive value of such scattering is responsible for the tendency for the gap function to assume opposite sign on the electron and hole pockets. However, on each Fermi surface the average magnitude of the gap function, the degrees of its variation as a function of angle, and whether it has node or not depend on the details of the band wave function as well as the values of the local interaction in our model. The present result confirms our earlier picture[5,20,31] of the antiferromagnetism-triggered pair scattering being the mechanism of superconductivity in the iron-based compounds. We believe that such mechanism should also at work in systems at the brim of band-insulator to semimetal phase transition (for example, as a function of pressure). On the semimetal side the charge count requires the electron and hole pockets to cover the same area (volume). If the centers of these pockets reside at time-reversal invariant $k$ points, then intrapocket pairing can take place. If the centers are not located at the time-reversal invariant points, then center-of-mass momentum zero Cooper pair will requires interpocket pairing (time reversal ensure such $k$ and $-k$ pockets exist). It become increasingly clear with time that the highest-$T_c$ compounds in the iron-based materials are not strongly correlating. This makes our method, the function renormalization group an unbiased, trustworthy method to study these systems. The neutron resonance and the quasiparticle interference experiments raise our hope that perhaps after all these years we finally understand an unconventional superconductor.

[1] I. I. Mazin, D. J. Singh, M. D. Johannes, and M. H. Du, Phys. Rev. Lett. **101**, 057003 (2008).

[2] K. Kuroki, S. Onari, R. Arita, H. Usui, Y. Tanaka, H. Kontani, and H. Aoki, Phys. Rev. Lett. **101**, 087004 (2008).

[3] Z.-J. Yao, J.-X. Li, and Z. D. Wang, New J. Phys. **11**, 025009 (2009).

[4] K. Seo, B. A. Bernevig, and J. Hu, Phys. Rev. Lett. **101**, 206404 (2008).

[5] F. Wang, H. Zhai, Y. Ran, A. Vishwanath, and D.-H. Lee, Phys. Rev. Lett. **102**, 047005 (2009).

[6] A. V. Chubukov, D. V. Efremov, and I. Eremin, Phys. Rev. B **78**, 134512 (2008).

[7] W.-Q. Chen, K.-Y. Yang, Y. Zhou, and F.-C. Zhang, Phys. Rev. Lett. **102**, 047006 (2009).

[8] Y. Wang, L. Shan, L. Fang, P. Cheng, C. Ren, and H.-H. Wen, Supercond. Sci. Technol. **22**, 015018 (2009); Y. Nakai, K. Ishida, Y. Kamihara, M. Hirano, and H. Hosono, J. Phys. Soc. Jpn. **77**, 073701 (2008); H.-J. Grafe, D. Paar, G. Lang, N. J. Curro, G. Behr, J. Werner, J. Hamann-Borrero, C. Hess, N. Leps, R. Klingeler, and B. Büchner, Phys. Rev. Lett. **101**, 047003 (2008); R. T. Gordon, N. Ni, C. Martin, M. A. Tanatar, M. D. Vannette, H. Kim, G. D. Samolyuk, J. Schmalian, S. Nandi, A. Kreyssig, A. I. Goldman, J. Q. Yan, S. L. Bud'ko, P. C. Canfield, and R. Prozorov, *ibid.* **102**, 127004 (2009)

[9] T. Y. Chen, Z. Tesanovic, R. H. Liu, X. H. Chen, and C. L. Chien, Nature (London) **453**, 1224 (2008); L. Malone, J. D. Fletcher, A. Serafin, A. Carrington, N. D. Zhigadlo, Z. Bukowski, S. Katrych, and J. Karpinski, Phys. Rev. B **79**, 140501(R) (2009); H. Ding, P. Richard, K. Nakayama, K. Sugawara, T. Arakane, Y. Sekiba, A. Takayama, S. Souma, T. Sato, T. Takahashi, Z. Wang, X. Dai, Z. Fang, G. F. Chen, J. L. Luo, and N. L. Wang, EPL **83**, 47001 (2008); T. Kondo, A. F. Santander-Syro, O. Copie, C. Liu, M. E. Tillman, E. D. Mun, J.

Schmalian, S. L. Bud'ko, M. A. Tanatar, P. C. Canfield, and A. Kaminski, Phys. Rev. Lett. **101**, 147003 (2008); K. Hashimoto, T. Shibauchi, S. Kasahara, K. Ikada, S. Tonegawa, T. Kato, R. Okazaki, C. J. van der Beek, M. Konczykowski, H. Takeya, K. Hirata, T. Terashima, and Y. Matsuda, *ibid.* **102**, 207001 (2009).

[10] C. C. Tsuei, J. R. Kirtley, C. C. Chi, Lock See Yu-Jahnes, A. Gupta, T. Shaw, J. Z. Sun, and M. B. Ketchen, Phys. Rev. Lett. **73**, 593 (1994).

[11] D. A. Wollman, D. J. Van Harlingen, W. C. Lee, D. M. Ginsberg, and A. J. Leggett, Phys. Rev. Lett. **71**, 2134 (1993).

[12] C. W. Hicks, T. M. Lippman, M. E. Huber, Z.-A. Ren, J. Yang, Z.-X. Zhao, and K. A. Moler, J. Phys. Soc. Jpn. **78**, 013708 (2009).

[13] T. A. Maier and D. J. Scalapino, Phys. Rev. B **78**, 020514(R) (2008).

[14] M. M. Korshunov and I. Eremin, Phys. Rev. B **78**, 140509(R) (2008).

[15] M. D. Lumsden, A. D. Christianson, D. Parshall, M. B. Stone, S. E. Nagler, G. J. MacDougall, H. A. Mook, K. Lokshin, T. Egami, D. L. Abernathy, E. A. Goremychkin, R. Osborn, M. A. McGuire, A. S. Sefat, R. Jin, B. C. Sales, and D. Mandrus, Phys. Rev. Lett. **102**, 107005 (2009).

[16] S. Chi, A. Schneidewind, J. Zhao, L. W. Harriger, L. Li, Y. Luo, G. Cao, Z. Xu, M. Loewenhaupt, J. Hu, and P. Dai, Phys. Rev. Lett. **102**, 107006 (2009).

[17] S. Li, Y. Chen, S. Chang, J. W. Lynn, L. Li, Y. Luo, G. Cao, Z. Xu, and P. Dai, Phys. Rev. B **79**, 174527 (2009).

[18] D. Inosov, J. Park, P. Bourges, D. Sun, Y. Sidis, A. Schneidewind, K. Hradil, D. Haug, C. Lin, B. Keimer, and V. Hinkov, Nat. Phys. **6**, 178 (2010).

[19] J. Zhao, L. Regnault, C. Zhang, M. Wang, Z. Li, F. Zhou, Z. Zhao, and P. Dai, arXiv:0908.0954 (unpublished).

[20] F. Wang, H. Zhai, and D.-H. Lee, EPL **85**, 37005 (2009).

[21] Q.-H. Wang and D.-H. Lee, Phys. Rev. B **67**, 020511(R) (2003).

[22] J. E. Hoffman, K. McElroy, D.-H. Lee, K. M. Lang, H. Eisaki, S. Uchida, and J. C. Davis, Science **297**, 1148 (2002); K. McElroy, R. W. Simmonds, J. E. Hoffman, D.-H. Lee, J. Orenstein, H. Eisaki, S. Uchida, and J. C. Davis, Nature (London) **422**, 592 (2003); J. C. Davis, Acta Phys. Pol. A **104**, 193 (2003); J. A. Slezak, J. Lee, and J. C. Davis, MRS Bull. **30**, 437 (2005); J. Lee, J. A. Slezak, and J. C. Davis, J. Phys. Chem. Solids **66**, 1370 (2005); T. Hanaguri, Y. Kohsaka, J. C. Davis, C. Lupien, I. Yamada, M. Azuma, M. Takano, K. Ohishi, M. Ono, and H. Takagi, Nat. Phys. **3**, 865 (2007); J. Lee, K. Fujita, A. R. Schmidt, C. K. Kim, H. Eisaki, S. Uchida, and J. C. Davis, Science **325**, 1099 (2009).

[23] T. Hanaguri, Y. Kohsaka, M. Ono, M. Maltseva, P. Coleman, I. Yamada, M. Azuma, M. Takano, K. Ohishi, and H. Takagi, Science **323**, 923 (2009).

[24] T. Hanaguri S. Niitaka, K. Kuroki, and H. Takagi, Science **328**, 474 (2010).

[25] J. D. Fletcher, A. Serafin, L. Malone, J. G. Analytis, J. H. Chu, A. S. Erickson, I. R. Fisher, and A. Carrington, Phys. Rev. Lett. **102**, 147001 (2009).

[26] C. W. Hicks, T. M. Lippman, M. E. Huber, J. G. Analytis, J. H. Chu, A. S. Erickson, I. R. Fisher, and K. A. Moler, Phys. Rev. Lett. **103**, 127003 (2009).

[27] J. K. Dong, T. Y. Guan, S. Y. Zhou, X. Qiu, L. Ding, C. Zhang, U. Patel, Z. L. Xiao, and S. Y. Li, Phys. Rev. B **80**, 024518 (2009).

[28] C. Michioka, H. Ohta, M. Matsui, J. Yang, K. Yoshimura, and M. Fang, arXiv:0911.3729 (unpublished).

[29] Y. Han, W. Y. Li, L. X. Cao, X. Y. Wang, B. Xu, B. R. Zhao, Y. Q. Guo, and J. L. Yang, Phys. Rev. Lett. **104**, 017003 (2010).

[30] T. A. Maier, S. Graser, D. J. Scalapino, and P. J. Hirschfeld, Phys. Rev. B **79**, 224510 (2009).

[31] H. Zhai, F. Wang, and D.-H. Lee, Phys. Rev. B **80**, 064517 (2009).

[32] K. Kuroki, H. Usui, S. Onari, R. Arita, and H. Aoki, Phys. Rev. B **79**, 224511 (2009).

[33] A. V. Chubukov, M. G. Vavilov, and A. B. Vorontsov, Phys. Rev. B **80**, 140515(R) (2009).

[34] R. Thomale, C. Platt, J. Hu, C. Honerkamp, and B. A. Bernevig, Phys. Rev. B **80**, 180505(R) (2009).

[35] K. Nakamura, R. Arita, and M. Imada, J. Phys. Soc. Jpn. **77**, 093711 (2008).

[36] A. Carrington, A. I. Coldea, J. D. Fletcher, N. E. Hussey, C. M. J. Andrew, A. F. Bangura, J. G. Analytis, J.-H. Chu, A. S. Erickson, I. R. Fisher, and R. D. McDonald, Physica C **469**, 459 (2009).

[37] D. H. Lu, M. Yi, S.-K. Mo, A. S. Erickson, J. Analytis, J.-H. Chu, D. J. Singh, Z. Hussain, T. H. Geballe, I. R. Fisher, and Z.-X. Shen, Nature (London) **455**, 81 (2008).

[38] The same conclusion is obtained by the authors of Ref. 32 (private communication).

[39] A. J. Williams, T. M. McQueen, and R. J. Cava, Solid State Commun. **149**, 1507 (2009).

[40] W. Bao, Y. Qiu, Q. Huang, M. A. Green, P. Zajdel, M. R. Fitzsimmons, M. Zhernenkov, S. Chang, M. Fang, B. Qian, E. K. Vehstedt, J. Yang, H. M. Pham, L. Spinu, and Z. Q. Mao, Phys. Rev. Lett. **102**, 247001 (2009).

[41] G. F. Chen, Z. G. Chen, J. Dong, W. Z. Hu, G. Li, X. D. Zhang, P. Zheng, J. L. Luo, and N. L. Wang, Phys. Rev. B **79**, 140509(R) (2009).

[42] Y. Xia, D. Qian, L. Wray, D. Hsieh, G. F. Chen, J. L. Luo, N. L. Wang, and M. Z. Hasan, Phys. Rev. Lett. **103**, 037002 (2009).

[43] T. Kariyado and M. Ogata, J. Phys. Soc. Jpn. **79**, 033703 (2010).